

The generic $U(1)_X$ models inspired from $SO(10)$

Tianjun Li,^{1,2,*} Qianfei Xiang,^{1,†} Xiangwei Yin,^{1,2,‡} and Han Zhou^{1,§}

¹*CAS Key Laboratory of Theoretical Physics, Institute of Theoretical Physics,
Chinese Academy of Sciences, Beijing 100190, China*

²*School of Physical Sciences, University of Chinese Academy of Sciences,
No. 19A Yuquan Road, Beijing 100049, China*

Abstract

We propose the family universal $U(1)_X$ models with three right-handed neutrinos by choosing the $U(1)_X$ gauge symmetry as a linear combination of $U(1)_Y \times U(1)_X$ of $SO(10)$. To be consistent with the quantum gravity effects, we introduced a Dirac fermion χ as a dark matter candidate, which is odd under the gauged Z_2 symmetry after $U(1)_X$ breaking. The isospin violation dark matter with $f_n/f_p = -0.7$ can be realized naturally, and thus the LUX, PANDAX, and XENON1T experimental constraints can be evaded. Moreover, we study the masses and mixings for Higgs and gauge bosons, consider the LHC constraints on the Z' mass, simulate various constraints from dark matter direct and indirect detection experiments, and then present the viable parameter spaces. To study the LHC Z' mass bounds on the generic $U(1)_X$ models, we considered four kinds of scenarios, where scenario II with zero $U(1)_X$ charge for right-handed up-type quarks can relax the LHC Z' mass bound a little bit.

* tli@itp.ac.cn

† xiangqf@pku.edu.cn

‡ yinxiangwei@itp.ac.cn

§ zhouhan@alumni.itp.ac.cn

I. INTRODUCTION

The Standard Model (SM) has been confirmed since Higgs particle was discovered at the LHC. However, there exist some evidences for new physics beyond the SM, for example, neutrino masses and mixings, dark matter (DM), dark energy, and cosmic inflation, etc. Therefore, the SM is not the whole story, and we need to explore the new physics. There are many possible directions to go beyond the SM. For example, the fine-tuning problem such as gauge hierarchy problem leads to supersymmetry [1], technicolor [2], extra dimensions [3, 4], etc, while the aesthetic issues such as the unification of fundamental interactions and the explanation of charge quantization lead to the grand unified theories (GUTs) [5] and string theory [6, 7].

On the other hand, DM particle candidates have a very wide mass range from around 10^{-22} eV to about $10M_{\odot}$ mass [8], including the weakly interacting massive particle (WIMP), the lightest supersymmetric particle (LSP), massive compact halo object (MACHO), super-heavy candidates, axino, sterile neutrino, fuzzy DM, and etc. Among these huge amount of DM candidates, WIMP is a well-motivated DM candidate. It is stable, nonrelativistic, electrically neutral, colorless, and have a mass range from about 10 GeV to few TeV. However, if the discrete symmetry, which stabilizes the DM candidate, is not a gauged discrete symmetry, it can be broken via the non-renormalizable operators due to quantum gravity effects, and then the DM candidate can decay and cannot be a valid DM candidate. Moreover, there are strong constraints from direct search experiments, for instance, the PandaX-II (2017) [9], LUX (2017) [10], and XENON1T (2018) [11] experiments. As we know, the isospin-violating dark matter (IVDM) is a kind of DM with different couplings f_p and f_n respectively to proton and neutron, and was originally proposed to explain the tensions among DAMA/LIBRA, CoGeNT, and XENON experiments for light DM [12, 13]. Interestingly, it can evade the LUX, PANDAX, and XENON1T experimental constraints naturally as well [14–16]. For these xenon based experiments [9–11], the ratio f_n/f_p is about -0.7 . Moreover, several IVDM models have been proposed in recent years [15, 17–24]. However, it is well known that in the $U(1)'$ models with E_6 origin, the vector coupling of the up-type quarks to the Z' boson should be zero while their axial coupling may have nonzero value. Thus, one cannot realize the isospin violation with $f_n/f_p = -0.7$ in the $U(1)'$ model from E_6 unless one introduces vectorlike particles [24].

In this paper, to explore the new physics beyond the SM, we choose a conservative approach by neglecting the fine-tuning and aesthetic problems, and concentrate on the low energy new physics [25]. In particular, we consider the family universal $U(1)_X$ models. If we only have SM fermions, the only $U(1)_X$ model, which one can build, is the top hypercharge model or its variation [26, 27]. Thus, we study the family universal $U(1)_X$ models with

SM particles	$2\sqrt{10}Q_\chi$	SM particles	$2\sqrt{10}Q_\chi$
Q_i, U_i^c, E_i^c	-1	D_i^c, L_i	3
N_i^c	-5	H	-2

TABLE I: The $U(1)_\chi$ charges of the SM particles.

three right-handed neutrinos in general, and then the neutrino masses and mixings can be explained via type I seesaw mechanism [28, 29]. As we know, one family of the SM fermions plus the right-handed neutrino forms a spinor representation **16** in $SO(10)$ model, and $SO(10)$ has a subgroup $SU(3)_C \times SU(2)_L \times U(1)_Y \times U(1)_\chi$. Therefore, we construct this kind of the $U(1)_X$ models by choosing the $U(1)_X$ gauge symmetry as a linear combination of $U(1)_Y \times U(1)_\chi$. For more discussions about generic and particular $U(1)$ models see [30]. Also, we introduce another Dirac fermion χ as a DM candidate, which is odd under the gauged Z_2 symmetry after $U(1)_X$ breaking. Thus, χ is a viable DM candidate consistent with the quantum gravity effects. Interestingly, we show that the isospin violation DM with $f_n/f_p = -0.7$ can be realized naturally in our models without introducing any vectorlike particles. Moreover, we study the masses and mixings for Higgs and gauge bosons, consider the LHC constraints on the Z' mass, simulate various constraints from DM direct and indirect detection experiments, and present the viable parameter spaces. To study the LHC Z' mass bounds on the generic $U(1)_X$ models, we consider four kinds of scenarios: scenarios I, II, and III have zero $U(1)_X$ charges, respectively, for quark doublets, right-handed up-type quarks, and right-handed down-type quarks, and scenario IV has approximately equal charges for all the quarks. We find that the low bounds on the Z' masses are about 4.94, 4.87, 5.34, and 5.09 TeV for scenarios I, II, III, and IV, respectively. Thus, scenario II can relax the LHC Z' mass bound a little bit, but not too much.

The this paper is organized as follows. In Sec II, we describe the $SO(10)$ -inspired $U(1)_X$ model, and calculate the Higgs mass and other parameters. In Sec III, we study the constraints from the LHC, dark matter direct and indirect detection experiments by considering isospin violation effects. In Sec IV, we discuss the LHC bounds on the Z' masses in four kind of scenarios. Finally, we conclude in Sec V.

II. THE GENERIC $U(1)_X$ MODELS INSPIRED FROM $SO(10)$

First, let us explain the convention. We denote the left-handed quark doublets, right-handed up-type quarks, right-handed down-type quarks, left-handed lepton doublets, right-handed neutrinos, right-handed charged leptons, and Higgs particle as $Q_i^c, U_i^c, D_i^c, L_i, N_i^c,$

Q_i	$(\mathbf{3}, \mathbf{2}, \mathbf{1}/6, \cos \alpha/6 - \sin \alpha/2\sqrt{10}, -1)$	U_i^c	$(\bar{\mathbf{3}}, \mathbf{1}, -\mathbf{2}/3, -2 \cos \alpha/3 - \sin \alpha/2\sqrt{10}, -1)$
D_i^c	$(\bar{\mathbf{3}}, \mathbf{1}, \mathbf{1}/3, \cos \alpha/3 + 3 \sin \alpha/2\sqrt{10}, \mathbf{3})$	L_i	$(\mathbf{1}, \mathbf{2}, -\mathbf{1}/2, -\cos \alpha/2 + 3 \sin \alpha/2\sqrt{10}, \mathbf{3})$
E_i^c	$(\mathbf{1}, \mathbf{1}, \mathbf{1}, \cos \alpha - \sin \alpha/2\sqrt{10}, -1)$	N_i^c	$(\mathbf{1}, \mathbf{1}, \mathbf{0}, -5 \sin \alpha/2\sqrt{10}, -5)$
H	$(\mathbf{1}, \mathbf{2}, -\mathbf{1}/2, -\cos \alpha/2 - 2 \sin \alpha/2\sqrt{10}, -\mathbf{2})$	S	$(\mathbf{1}, \mathbf{1}, \mathbf{0}, 10 \sin \alpha/2\sqrt{10}, \mathbf{10})$

TABLE II: The particles and their quantum numbers under the $SU(3)_C \times SU(2)_L \times U(1)_Y \times U(1)_X$ and $U(1)_X$ gauge symmetry. Here, the correct $U(1)_X$ charges are the $U(1)_X$ charges in the above Table divided by $2\sqrt{10}$.

E_i^c , and H , respectively. As we know, the $SO(10)$ gauge symmetry can be broken down to the $SU(3)_C \times SU(2)_L \times U(1)_Y \times U(1)_X$ gauge symmetry [31–38], where $U(1)_X$ charges for the SM particles are given in Table I.

We shall propose the generic $U(1)_X$ model inspired from $SO(10)$, which is the mixing between the previous $U(1)_X$ gauge symmetry and $U(1)_Y$ gauge symmetry. Thus, we have

$$Q_X = \cos \alpha Q_Y + \sin \alpha Q_X. \quad (1)$$

To break $U(1)_X$ gauge symmetry and give masses to the right-handed neutrinos, we introduce a SM singlet Higgs S with $U(1)_X$ charge 10. So the neutrino masses can be explained via the type I seesaw mechanism. The particles and their quantum numbers under the $SU(3)_C \times SU(2)_L \times U(1)_Y \times U(1)_X$ gauge symmetry are given in Table II.

Assuming the interactions between the DM and nucleons are mediated by the $U(1)_X$ gauge boson, we obtain the coupling ratio f_n/f_p in our model

$$f_n/f_p = \frac{b_u + 2b_d}{2b_u + b_d} = \frac{(q_Q - q_{U^c}) + 2(q_Q - q_{D^c})}{2(q_Q - q_{U^c}) + (q_Q - q_{D^c})}, \quad (2)$$

where q_f represents the corresponding $U(1)_X$ charge for particle f , which is given in Table II. Thus, we have

$$f_n/f_p = \frac{\sqrt{10} \cos \alpha - 8 \sin \alpha}{3\sqrt{10} \cos \alpha - 4 \sin \alpha}. \quad (3)$$

To have $f_n/f_p = -0.7$, we obtain $\tan \alpha = \frac{31}{108}\sqrt{10}$. Therefore, the $U(1)_X$ charges of the SM particles can be calculated, and are presented in the Table III. To be consistent with GUTs, we choose $g_X \simeq \sqrt{5/3}g_Y$, and assume that the contribution to the one-loop beta function of $U(1)_X$ from one family of the SM fermions in the supersymmetric $U(1)_X$ models is equal to 2 as in the supersymmetric SMs or GUTs. Thus, we obtain the following normalization factor of $U(1)_X$ charge

$$N = \sqrt{\frac{Q_i^2 \times 2 \times 3 + U_i^2 \times 1 \times 3 + D_i^2 \times 1 \times 3 + L_i^2 \times 2 + E_i^2 \times 1 + N_i^2 \times 1}{2}}. \quad (4)$$

Q_i	$(\mathbf{3}, \mathbf{2}, \mathbf{1}/\mathbf{6}, \mathbf{1}, -\mathbf{1})$	U_i^c	$(\bar{\mathbf{3}}, \mathbf{1}, -\mathbf{2}/\mathbf{3}, -\mathbf{35}, -\mathbf{1})$
D_i^c	$(\bar{\mathbf{3}}, \mathbf{1}, \mathbf{1}/\mathbf{3}, \mathbf{33}, \mathbf{3})$	L_i	$(\mathbf{1}, \mathbf{2}, -\mathbf{1}/\mathbf{2}, -\mathbf{3}, \mathbf{3})$
E_i^c	$(\mathbf{1}, \mathbf{1}, \mathbf{1}, \mathbf{37}, -\mathbf{1})$	N_i^c	$(\mathbf{1}, \mathbf{1}, \mathbf{0}, -\mathbf{31}, -\mathbf{5})$
H	$(\mathbf{1}, \mathbf{2}, -\mathbf{1}/\mathbf{2}, -\mathbf{34}, -\mathbf{2})$	S	$(\mathbf{1}, \mathbf{1}, \mathbf{0}, \mathbf{62}, \mathbf{10})$
χ	$(\mathbf{1}, \mathbf{1}, \mathbf{0}, \mathbf{31}/\mathbf{2}, \mathbf{5}/\mathbf{2})$		

TABLE III: The particles and their quantum numbers under the $SU(3)_C \times SU(2)_L \times U(1)_Y \times U(1)_X$ and $U(1)_\chi$ gauge symmetry. Here, the correct $U(1)_\chi$ and $U(1)_X$ charges are their charges in the above table divided by $2\sqrt{10}$ and $2\sqrt{1162}$.

Moreover, we introduce a Dirac fermion χ as DM candidate, whose $U(1)_X$ charge is a half integer. Of course, there are many choices for its $U(1)_X$ charge, and we take $31/2$ for simplicity, which is given in the table as well.

The Lagrangian is given by

$$\begin{aligned}
-\mathcal{L} = & m_S^2 |S|^2 + m_H^2 |H|^2 + \frac{\lambda_S}{2} |S|^4 + \frac{\lambda_H}{2} |H|^4 + \lambda_{SH} |S|^2 |H|^2 + \left(y_{ij}^U Q_i U_j^c \tilde{H} \right. \\
& \left. + y_{ij}^D Q_i D_j^c H + y_{ij}^E L_i E_j^c H + y_{ij}^N L_i N_j^c \tilde{H} + y_{ij}^{MN} S N_i^c N_j^c + \text{H.C.} \right) , \quad (5)
\end{aligned}$$

where $\tilde{H} = i\sigma_2 H^*$.

We parametrize the Higgs fields as follows:

$$S = v_s + S_1 + iS_2 \quad , \quad H = \begin{pmatrix} H^+ \\ v_h + H_1 + iH_2 \end{pmatrix} . \quad (6)$$

After gauge symmetry breakings, the vacuum expectation values (VEVs) of these Higgs fields are given by

$$\langle S \rangle = v_s \quad , \quad \langle H \rangle = \begin{pmatrix} 0 \\ v_h \end{pmatrix} . \quad (7)$$

We have four Nambu-Goldstone bosons from H^\pm , H_2 , and S_2 , as well as two neutral physical scalars s and h from the mixings of S_1 and H_1 via their following mass matrix

$$M_{(S_1, H_1)} = \begin{bmatrix} 2v_s^2 \lambda_S & 2v_h v_s \lambda_{SH} \\ 2v_h v_s \lambda_{SH} & 2v_h^2 \lambda_H \end{bmatrix} . \quad (8)$$

The physical scalars s and h can be written as the linear combination of H_1 and S_1

$$\begin{pmatrix} s \\ h \end{pmatrix} = \begin{pmatrix} \cos \theta & -\sin \theta \\ \sin \theta & \cos \theta \end{pmatrix} \begin{pmatrix} S_1 \\ H_1 \end{pmatrix} , \quad (9)$$

where the mixing angle θ is

$$\tan 2\theta = \frac{2v_h v_s \lambda_{SH}}{v_h^2 \lambda_H - v_s^2 \lambda_S}. \quad (10)$$

The Higgs masses are, respectively,

$$m_{s/h}^2 = \lambda_h v_h^2 + \lambda_s v_s^2 \pm \sqrt{4\lambda_{sh}^2 v_h^2 v_s^2 - 2\lambda_s \lambda_h v_h^2 v_s^2 + \lambda_h^2 v_h^4 + \lambda_s^2 v_s^4}. \quad (11)$$

Because h is the SM Higgs field, we should have $v_h = 174$ GeV and $m_h = 125$ GeV.

Next we shall discuss the gauge boson masses. The covariant derivative in our model is

$$\begin{aligned} D_\mu &= \partial_\mu - ig_2 T^i A_\mu^i - ig_Y Y B_\mu - ig_X X C_\mu \\ &= \partial_\mu - i \begin{pmatrix} \frac{1}{2} g_2 A_\mu^3 - \frac{1}{2} g_Y B_\mu + g_X X C_\mu & \frac{g_2 W_\mu^+}{\sqrt{2}} \\ \frac{g_2 W_\mu^-}{\sqrt{2}} & -\frac{1}{2} g_2 A_\mu^3 - \frac{1}{2} g_Y B_\mu + g_X X C_\mu \end{pmatrix}, \end{aligned} \quad (12)$$

where $i = 1, 2, 3$, T^i are the three generators of $SU(2)_L$, Y and X are the charges, respectively for $U(1)_Y$ and $U(1)_X$, g_2 , g_Y and g_X are the gauge couplings, respectively, for $SU(2)_L$, $U(1)_Y$, and $U(1)_X$, W_μ^\pm are the SM charged gauge bosons $W_\mu^\pm = \frac{A_\mu^1 \mp i A_\mu^2}{\sqrt{2}}$, A_μ^i and B_μ are the SM gauge fields, and C_μ represents for the $U(1)_X$ gauge field.

After gauge symmetry breaking, we obtain the gauge boson masses from the kinetic terms of the Higgs fields

$$\begin{aligned} \mathcal{L}_{GM} &= (D_\mu H)^\dagger D_\mu H + (D_\mu S)^\dagger D_\mu S \\ &\stackrel{\text{VEV}}{=} v_h^2 \left(-\frac{1}{2} g_2 A_\mu^3 - \frac{1}{2} g_Y B_\mu + g_X X C_\mu \right)^2 + v_s^2 g_X^2 C_\mu^2 X_s^2 + \frac{1}{2} g_2^2 v_h^2 W_\mu^+ W^{-\mu}. \end{aligned} \quad (13)$$

The gauge boson mass matrix in the basis (A_μ^3, B_μ, C_μ) is

$$\begin{pmatrix} \frac{1}{2} g_2^2 v_h^2 & \frac{1}{2} g_2 g_Y v_h^2 & -g_2 g_X v_h^2 X_h \\ \frac{1}{2} g_2 g_Y v_h^2 & \frac{1}{2} g_Y^2 v_h^2 & -g_Y g_X v_h^2 X_h \\ -g_2 g_X v_h^2 X_h & -g_Y g_X v_h^2 X_h & 2g_X^2 v_h^2 X_h^2 + 2g_X^2 v_s^2 X_s^2 \end{pmatrix}, \quad (14)$$

and then the gauge boson mass are given by

$$\begin{aligned} m_1^2 &= 0, \quad m_{2,3}^2 = \frac{1}{4} \left(g_2^2 v_h^2 + g_Y^2 v_h^2 + 4g_X^2 v_h^2 X_h^2 + 4g_X^2 v_s^2 X_s^2 \right. \\ &\quad \left. \pm \sqrt{(-g_2^2 v_h^2 - g_Y^2 v_h^2 - 4g_X^2 v_h^2 X_h^2 - 4g_X^2 v_s^2 X_s^2)^2 - 4(4g_2^2 g_X^2 v_h^2 v_s^2 X_s^2 + 4g_Y^2 g_X^2 v_h^2 v_s^2 X_s^2)} \right), \end{aligned} \quad (15)$$

which obviously are the masses for photon, Z , and Z' gauge bosons, respectively. Because Z' is much heavier than Z , we have $m_3^2 = m_Z^2$. With these calculations, we can give these parameters the proper values to satisfy the experimental constraints. For example, we can

have $v_s = 8000$ GeV, $m_H = 1884$ GeV, $m_S = 3465$ GeV, $\lambda_S = 0.17$, $\lambda_H = 0.27$, $\lambda_{SH} = 0.05$, $g_X = 0.50$, and then get $m_h = 125$ GeV, $m_s = 4900$ GeV, and $m_{Z'} = 5500$ GeV.

At low energy, we have the SM particles, Z' , and DM χ . Therefore, we can use the simplified $U(1)_X$ model whose the interactions are given by

$$-\mathcal{L} = \sum_q g_u \bar{u} \gamma^\mu u Z'_\mu + g_{uA} \bar{u} \gamma^\mu \gamma^5 u Z'_\mu + g_d \bar{d} \gamma^\mu d Z'_\mu + g_{dA} \bar{d} \gamma^\mu \gamma^5 d Z'_\mu + g_\chi \bar{\chi} \gamma^\mu \chi Z'_\mu, \quad (16)$$

Where $g_f = g_X q_f$ with q_f the $U(1)_X$ charge for the fermion f , and we have

$$g_u : g_d : g_{uA} : g_{dA} : g_\chi = 36 : -32 : 34 : -34 : 31, \quad q_u = 18/\sqrt{1162}. \quad (17)$$

III. THE $U(1)_X$ MODEL WITH THE IVDM χ

First, we would like to study the LHC constraints on the Z' mass via the code Z' explorer [39]. For simplicity, we take $g_X = \sqrt{\frac{5}{3}} g_Y = 0.46$, and then we have $g_{uL} = g_{dL} \approx 0.0067$, $g_{uR} \approx 0.236$, and $g_{dR} \approx -0.223$. Further parameter settings can be found in the Appendix A. Because the $U(1)_X$ charge of Q_i is much smaller than U_i^c and D_i^c , the coupling between the left-handed quarks and Z' is much smaller than the right-handed quarks.

We present the LHC simulation results in Fig. 1. $S = \frac{\sigma_{pred}}{\sigma_{lim}}$ is the signal strength for each channel, where σ_{pred} is the predicted Z' production cross section times branching ratio times acceptance and σ_{lim} is the corresponding predicted experimental upper limit at the 95% confidence level (C.L). If $S > 1$, then the corresponding point in the parameter space is experimentally excluded. If $S < 1$ for all channels, then the corresponding point is viable. Therefore, the channels with the $e\bar{e}$ and $\mu\bar{\mu}$ final states give the strong constraints on Z' mass, and we obtain that the low bound on Z' mass in our model is around 5.03 TeV. Because the current LHC mass bound on generic Z' is about 5 TeV [40], our numerical result is consistent with LHC searches. For simplicity, we shall take $M_{Z'} = 5.5$ TeV in the following study.

Second, we shall consider the direct and indirect experimental constraints on the DM χ , and present the simulation results in the g_X versus m_χ plane with $M_{Z'} = 5.5$ TeV and in the $M_{Z'}$ versus m_χ plane with $g_X = 0.46$, respectively, in the left and right panels of Fig. 2. In the left panel, to have the decay width of Z' smaller than Z' mass from the Z' particle point of view, we obtain that the upper bound on g_X is roughly 2, *i.e.*, $g_X < 2$. In the right panel, we have the low bound on Z' mass from the LHC constraints, *i.e.*, $m_{Z'} > 5.03$ TeV. These two conditions are shown as the solid black lines in Fig. 2. Also, the dark-green line indicates the parameter space with the observed dark matter relic density, *i.e.*, $\Omega_\chi h^2 = 0.12$ and the relic density is calculated by the popular code MicrOMEGAs [45, 46].

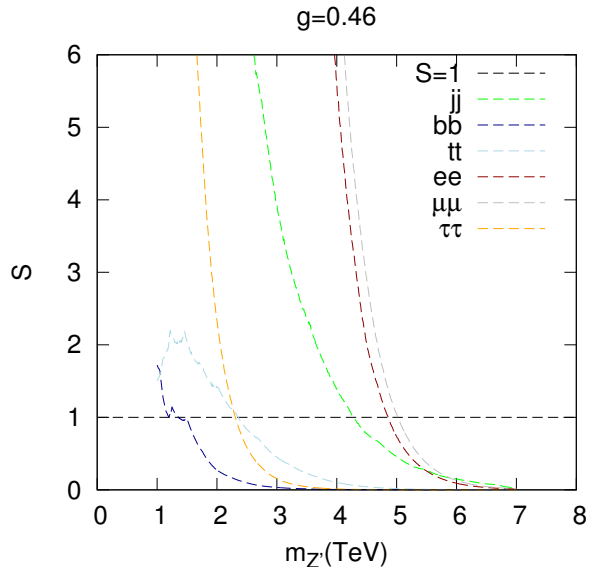


FIG. 1: The signal strengths of the SM fermion final states versus Z' mass for the Z' searches at the LHC. The LHC bound on the Z' mass is about 5.03 TeV.

The solid purple, orange and yellow lines, respectively, correspond to the constraints from the PandaX-II (2017) [9], Xenon1T (2018) [11], and DEAP3600 (2019) [41] experiments. The first two experiments are xenon-based DM direct detections, while the last one is argon-based. On account of isospin-violating affects, they have the rescale factors around 7600 and 235 [42], respectively. Compared to the two black lines, the DM direct detection experiments barely give additional constraints, and then we have escaped these experimental constraints.

The dashed blue and red lines correspond to the constraints from the Fermi-dSph (6 year) [43] and HESS (254h) [44], respectively. In addition, we should clarify that the DAMA and GoGeNT are not shown, since they have less constrains. The interesting parameter spaces for our simulations are distributed in the resonant regions, which have $m_\chi \sim \frac{1}{2}m_{Z'}$, and these regions together with the regions below the black lines constitute the main parameter spaces in our model.

Comparing the direct and indirect experiments, we find that the indirect detection have much better sensitivity near the resonant regions with $m_\chi \sim \frac{1}{2}m_{Z'}$ due to resonant enhancement. Beyond these regions, the direct detection experiments have better sensitivities. In short, there are still some viable parameter spaces in our $U(1)_X$ model.

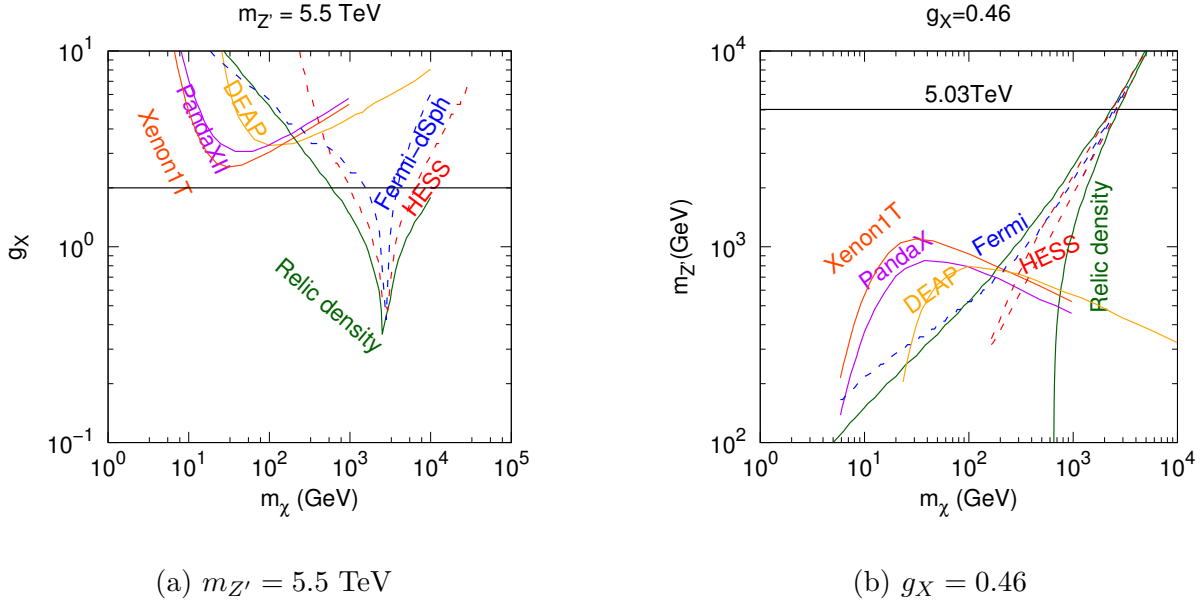


FIG. 2: Exclusion line for direct detection experiments and indirect detection experiments.

IV. THE GENERIC $U(1)_X$ MODELS WITH LHC BOUNDS ON THE Z' MASSES

In the following, we shall consider four scenarios and study the LHC low bounds on the Z' mass.

A. Scenario I: The $U(1)_X$ model with zero $U(1)_X$ charge for the quark doublets Q_i

In scenario I, we consider that the $U(1)_X$ charge for the quark doublets Q_i is equal to 0, and then we obtain

$$\tan \alpha = \frac{\sqrt{10}}{3}. \quad (18)$$

The particles and their quantum numbers under the $SU(3)_C \times SU(2)_L \times U(1)_Y \times U(1)_X$ gauge symmetry are given in Table IV. We present the LHC simulation results in Fig. 3, and obtain that low bound on Z' boson mass is about 4.94 TeV.

B. Scenario II: The $U(1)_X$ model with zero $U(1)_X$ charge for the right-handed up-type quarks U_i^c

In scenario II, we consider that the $U(1)_X$ charge for the right-handed up-type quarks U_i^c is equal to 0, and then we obtain

$$\tan \alpha = -\frac{4\sqrt{10}}{3}. \quad (19)$$

Q_i	$(\mathbf{3}, \mathbf{2}, \mathbf{1}/\mathbf{6}, \mathbf{0}, -\mathbf{1})$	U_i^c	$(\bar{\mathbf{3}}, \mathbf{1}, -\mathbf{2}/\mathbf{3}, \mathbf{1}, -\mathbf{1})$
D_i^c	$(\bar{\mathbf{3}}, \mathbf{1}, \mathbf{1}/\mathbf{3}, -\mathbf{1}, \mathbf{3})$	L_i	$(\mathbf{1}, \mathbf{2}, -\mathbf{1}/\mathbf{2}, \mathbf{0}, \mathbf{3})$
E_i^c	$(\mathbf{1}, \mathbf{1}, \mathbf{1}, -\mathbf{1}, -\mathbf{1})$	N_i^c	$(\mathbf{1}, \mathbf{1}, \mathbf{0}, \mathbf{1}, -\mathbf{5})$
H	$(\mathbf{1}, \mathbf{2}, -\mathbf{1}/\mathbf{2}, \mathbf{1}, -\mathbf{2})$	S	$(\mathbf{1}, \mathbf{1}, \mathbf{0}, -\mathbf{2}, \mathbf{10})$

TABLE IV: The particles and their quantum numbers under the $SU(3)_C \times SU(2)_L \times U(1)_Y \times U(1)_X$ and $U(1)_X$ gauge symmetry in scenario I. Here, the correct $U(1)_X$ and $U(1)_X$ charges are their charges in the above table divided by $2\sqrt{10}$ and 2.

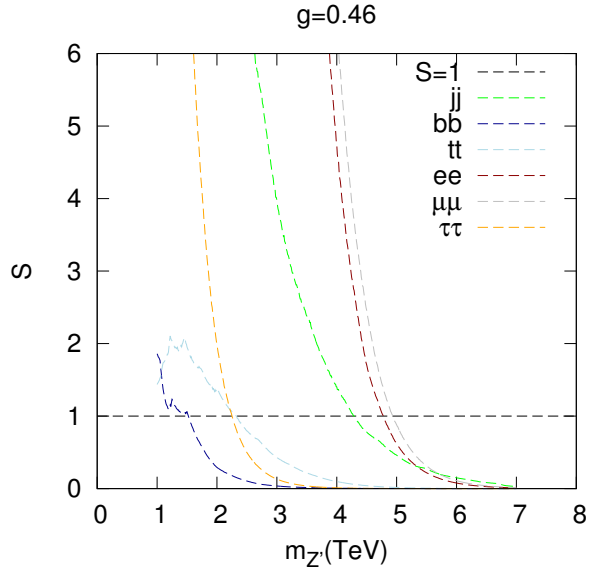


FIG. 3: The signal strengths of the SM fermion final states versus Z' mass for the Z' searches at the LHC in scenario I. The low bound on Z' mass is around 4.94 TeV.

The particles and their quantum numbers under the $SU(3)_C \times SU(2)_L \times U(1)_Y \times U(1)_X$ gauge symmetry are given in Table V. We present the LHC simulation results in Fig. 4, and obtain that low bound on Z' boson mass is about 4.87 TeV.

Q_i	$(\mathbf{3}, \mathbf{2}, \mathbf{1}/\mathbf{6}, \mathbf{1}, -\mathbf{1})$	U_i^c	$(\bar{\mathbf{3}}, \mathbf{1}, -\mathbf{2}/\mathbf{3}, \mathbf{0}, -\mathbf{1})$
D_i^c	$(\bar{\mathbf{3}}, \mathbf{1}, \mathbf{1}/\mathbf{3}, -\mathbf{2}, \mathbf{3})$	L_i	$(\mathbf{1}, \mathbf{2}, -\mathbf{1}/\mathbf{2}, -\mathbf{3}, \mathbf{3})$
E_i^c	$(\mathbf{1}, \mathbf{1}, \mathbf{1}, \mathbf{2}, -\mathbf{1})$	N_i^c	$(\mathbf{1}, \mathbf{1}, \mathbf{0}, \mathbf{4}, -\mathbf{5})$
H	$(\mathbf{1}, \mathbf{2}, -\mathbf{1}/\mathbf{2}, \mathbf{1}, -\mathbf{2})$	S	$(\mathbf{1}, \mathbf{1}, \mathbf{0}, -\mathbf{8}, \mathbf{10})$

TABLE V: The particles and their quantum numbers under the $SU(3)_C \times SU(2)_L \times U(1)_Y \times U(1)_X$ and $U(1)_X$ gauge symmetry in scenario II. Here, the correct $U(1)_X$ and $U(1)_X$ charges are their charges in the above table divided by $2\sqrt{10}$ and $2\sqrt{7}$.

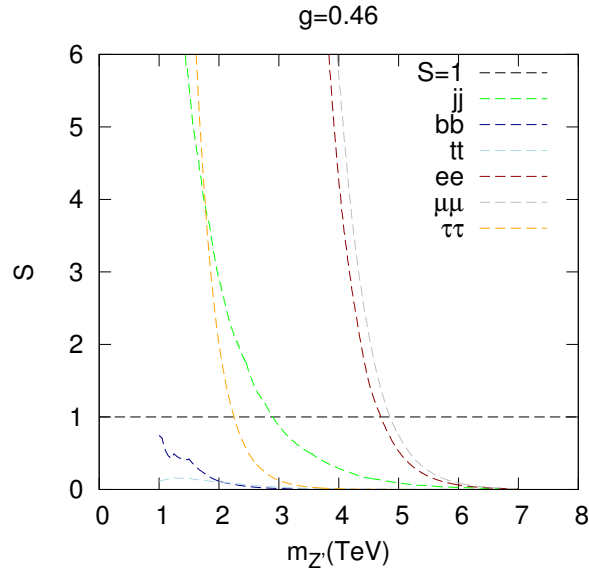


FIG. 4: The signal strengths of the SM fermion final states versus Z' mass for the Z' searches at the LHC in scenario II. The low bound on Z' mass is around 4.87 TeV.

C. Scenario III: The $U(1)_X$ model with zero $U(1)_X$ charge for the right-handed down-type quarks D_i^c

In scenario III, we consider that the $U(1)_X$ charge for the right-handed down-type quarks D_i^c is equal to 0, and then we obtain

$$\tan \alpha = -\frac{2\sqrt{10}}{9}. \quad (20)$$

The particles and their quantum numbers under the $SU(3)_C \times SU(2)_L \times U(1)_Y \times U(1)_X$ gauge symmetry are given in Table VI. We present the LHC simulation results in Fig. 5, and obtain that the low bound on the Z' boson mass is about 5.34 TeV.

Q_i	$(\mathbf{3}, \mathbf{2}, \mathbf{1/6}, \mathbf{1}, -\mathbf{1})$	U_i^c	$(\bar{\mathbf{3}}, \mathbf{1}, -\mathbf{2/3}, -\mathbf{2}, -\mathbf{1})$
D_i^c	$(\bar{\mathbf{3}}, \mathbf{1}, \mathbf{1/3}, \mathbf{0}, \mathbf{3})$	L_i	$(\mathbf{1}, \mathbf{2}, -\mathbf{1/2}, -\mathbf{3}, \mathbf{3})$
E_i^c	$(\mathbf{1}, \mathbf{1}, \mathbf{1}, \mathbf{4}, -\mathbf{1})$	N_i^c	$(\mathbf{1}, \mathbf{1}, \mathbf{0}, \mathbf{2}, -\mathbf{5})$
H	$(\mathbf{1}, \mathbf{2}, -\mathbf{1/2}, -\mathbf{1}, -\mathbf{2})$	S	$(\mathbf{1}, \mathbf{1}, \mathbf{0}, -\mathbf{4}, \mathbf{10})$

TABLE VI: The particles and their quantum numbers under the $SU(3)_C \times SU(2)_L \times U(1)_Y \times U(1)_X$ and $U(1)_X$ gauge symmetry in scenario III. Here, the correct $U(1)_Y$ and $U(1)_X$ charges are their charges in the above table divided by $2\sqrt{10}$ and $2\sqrt{7}$.

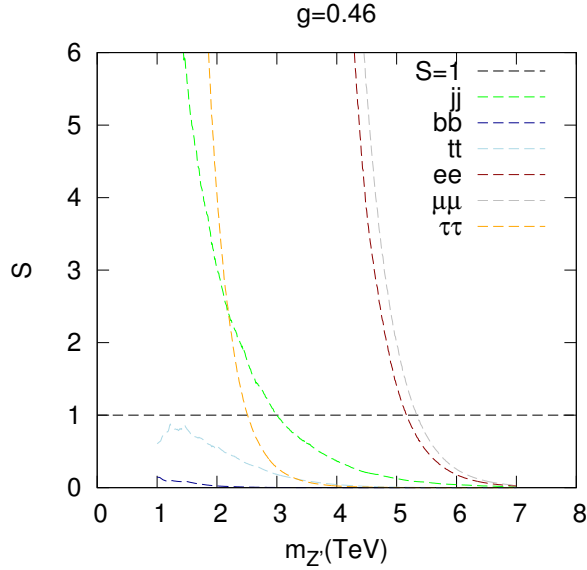


FIG. 5: The signal strengths of the SM fermion final states versus Z' mass for the Z' searches at the LHC in scenario III. The low bound on Z' boson mass is around 5.34 TeV.

D. Scenario IV: The $U(1)_X$ model with approximately equal $U(1)_X$ charges for the quark doublets Q_i , right-handed up-type quarks U_i^c , and right-handed down-type quarks D_i^c

In scenario IV, we consider that the $U(1)_X$ charge for the quark doublets Q_i , right-handed up-type quarks U_i^c and right-handed down-type quarks D_i^c are approximately equal, and then we obtain

$$\tan \alpha = -\sqrt{\frac{13}{5}}. \quad (21)$$

The particles and their quantum numbers under the $SU(3)_C \times SU(2)_L \times U(1)_Y \times U(1)_X$ gauge symmetry are given in Table VII. We present the LHC simulation results in Fig. 6,

and obtain that low bound on Z' boson mass is about 5.09 TeV. Therefore, scenario II can relax the LHC Z' mass bound a little bit.

Q_i	$(\mathbf{3}, \mathbf{2}, \mathbf{1}/\mathbf{6}, \mathbf{1}, -\mathbf{1})$	U_i^c	$(\bar{\mathbf{3}}, \mathbf{1}, -\mathbf{2}/\mathbf{3}, \frac{317-75\sqrt{26}}{67}, -\mathbf{1})$
D_i^c	$(\bar{\mathbf{3}}, \mathbf{1}, \mathbf{1}/\mathbf{3}, \frac{75\sqrt{26}-451}{67}, \mathbf{3})$	L_i	$(\mathbf{1}, \mathbf{2}, -\mathbf{1}/\mathbf{2}, -\mathbf{3}, \mathbf{3})$
E_i^c	$(\mathbf{1}, \mathbf{1}, \mathbf{1}, \frac{75\sqrt{26}-183}{67}, -\mathbf{1})$	N_i^c	$(\mathbf{1}, \mathbf{1}, \mathbf{0}, \frac{585-75\sqrt{26}}{67}, -\mathbf{5})$
H	$(\mathbf{1}, \mathbf{2}, -\mathbf{1}/\mathbf{2}, \frac{384-75\sqrt{26}}{67}, -\mathbf{2})$	S	$(\mathbf{1}, \mathbf{1}, \mathbf{0}, \frac{150\sqrt{26}-1170}{67}, \mathbf{10})$

TABLE VII: The particles and their quantum numbers under the $SU(3)_C \times SU(2)_L \times U(1)_Y \times U(1)_X$ and $U(1)_\chi$ gauge symmetry in scenario IV. Here, the correct $U(1)_\chi$ and $U(1)_X$ charges are their charges in the above table divided by $2\sqrt{10}$ and $\frac{16\sqrt{5010-900\sqrt{26}}}{67}$.

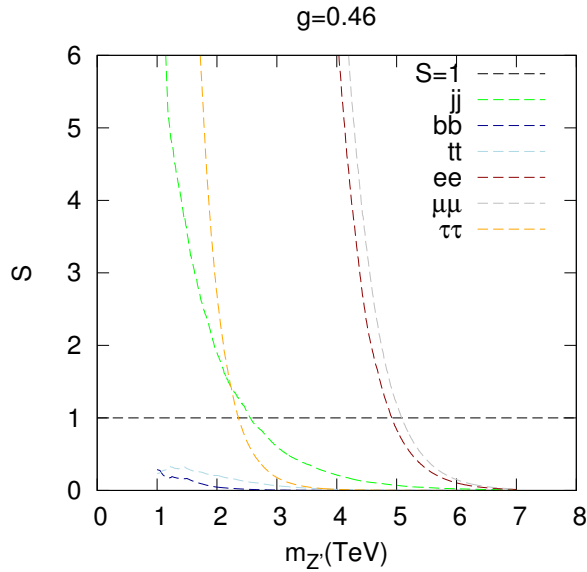


FIG. 6: The signal strengths of the SM fermion final states versus Z' mass for the Z' searches at the LHC in scenario IV. The low bound on Z' mass is around 5.09 TeV.

V. CONCLUSION

We constructed the family universal $U(1)_X$ models with three right-handed neutrinos by choosing the $U(1)_X$ gauge symmetry as a linear combination of $U(1)_Y \times U(1)_\chi$ of $SO(10)$. To be consistent with the quantum gravity effects, we introduced a Dirac fermion χ as a DM candidate, which is odd under the gauged Z_2 symmetry after $U(1)_X$ breaking. To satisfy

the LUX, PANDAX, and XENON1T experimental constraints, we found that the isospin violation DM with $f_n/f_p = -0.7$ can be realized naturally. In addition, we studied the masses and mixings for Higgs and gauge bosons, considered the LHC constraints on the Z' mass, simulated various constraints from DM direct and indirect detection experiments, and then presented the viable parameter spaces. To study the LHC Z' mass bounds on the generic $U(1)_X$ models, we considered four kinds of scenarios: scenarios I, II, and III have zero $U(1)_X$ charges, respectively, for quark doublets, right-handed up-type quarks, and right-handed down-type quarks, and scenario IV has approximately equal charges for all the quarks. We found that the LHC low bounds on the Z' masses are about 4.94, 4.87, 5.34, and 5.09 TeV for scenarios I, II, III, and IV, respectively. Thus, scenario II can relax the LHC Z' mass bound a little bit.

ACKNOWLEDGMENTS

This work is supported in part by the National Key Research and Development Program of China Grant No. 2020YFC2201504, by the Projects No. 11875062, No. 11947302, No. 12047503, and No. 12275333 supported by the National Natural Science Foundation of China, by the Key Research Program of the Chinese Academy of Sciences, Grant NO. XDPB15, by the Scientific Instrument Developing Project of the Chinese Academy of Sciences, Grant No. YJKYYQ20190049, and by the International Partnership Program of Chinese Academy of Sciences for Grand Challenges, Grant No. 112311KYSB20210012.

Appendix A: Z' Decay Widths

We present the Z' decay widths in details for Sec.III. The vacuum value v_s can be written as

$$v_s^2 = \frac{2M_Z^4 - M_Z^2 v_h^2 (g_2^2 + g_Y^2 + 4g_X^2 X_h^2)}{2g_X^2 (2M_Z^2 - (g_2^2 + g_Y^2) v_h^2) X_s^2}. \quad (\text{A1})$$

The decay widths of Z' to W^+W^- and to Zh are, respectively,

$$\begin{aligned} & \Gamma(Z' \rightarrow W^+W^-) \\ &= \frac{g_2^2}{192\pi} \cos^2(\theta_W) \sin^2(\theta_X) M_{Z'} \left(\frac{M_{Z'}}{M_Z}\right)^4 \left(1 - 4\frac{M_W^2}{M_{Z'}^2}\right)^{3/2} \left(1 + 20\frac{M_W^2}{M_{Z'}^2} + 12\frac{M_W^4}{M_{Z'}^4}\right), \end{aligned} \quad (\text{A2})$$

$$\begin{aligned} & \Gamma(Z' \rightarrow Zh) \\ &= \frac{g_2^2 M_Z^2}{192\pi M_W^2} M_{Z'} \sqrt{\lambda} \left(\lambda + 12\frac{M_Z^2}{M_{Z'}^2}\right) \left[\left(\frac{4M_Z^2}{v_h^2} - g_X^2\right) \sin(2\theta_X) + \left(\frac{4M_Z^2 g_X^2}{v_h^2}\right) \cos(2\theta_X)\right], \end{aligned} \quad (\text{A3})$$

where

$$\lambda = 1 + \left(\frac{M_Z^2}{M_{Z'}^2}\right)^2 + \left(\frac{M_h^2}{M_{Z'}^2}\right)^2 - 2\left(\frac{M_Z^2}{M_{Z'}^2}\right) - 2\left(\frac{M_h^2}{M_{Z'}^2}\right) - 2\left(\frac{M_Z^2}{M_{Z'}^2}\right)\left(\frac{M_h^2}{M_{Z'}^2}\right). \quad (\text{A4})$$

For our model, θ_X is the $Z-Z'$ mixing angle, which is very small, so we have $\sin(\theta_X) \approx \theta_X$, $\cos(\theta_X) \approx 1$, and

$$\sin(\theta_X) = \sqrt{\frac{A-B}{2A}}, \quad (\text{A5})$$

where A and B are defined by

$$\begin{aligned} A &= \sqrt{v_h^4 (g_2^2 + g_Y^2 + 4g_X^2 X_h^2)^2 - 8g_X^2 v_h^2 v_s^2 (g_2^2 + g_Y^2 - 4g_X^2 X_h^2) X_s^2 + 16g_X^4 v_s^4 X_s^4} \\ B &= 4g_X^2 v_s^2 X_s^2 - v_h^2 (g_2^2 + g_Y^2 - 4g_X^2 X_h^2). \end{aligned} \quad (\text{A6})$$

For DM annihilation cross sections calculation, we also need Z' decay widths to $\chi\chi$ and $q\bar{q}$

$$\Gamma_{Z'} = \Gamma(Z' \rightarrow \chi\bar{\chi}) + \sum_q c_q \Gamma(Z' \rightarrow q\bar{q}), \quad (\text{A7})$$

with

$$\Gamma(Z' \rightarrow q\bar{q}) = \frac{m_{Z'}}{12\pi} (g_{qA}^2 \xi_q (1 + \frac{2m_q^2}{m_{Z'}^2}) + g_{qV}^2 \xi_q^3), \quad (\text{A8})$$

$$\Gamma(Z' \rightarrow \chi\bar{\chi}) = \frac{m_{Z'}}{12\pi} g_\chi^2 (\xi_\chi (1 + \frac{2m_\chi^2}{m_{Z'}^2}) + \xi_\chi^3). \quad (\text{A9})$$

-
- [1] S. Dimopoulos and S. Raby, Nucl. Phys. B **192**, 353 (1981); E. Witten, Nucl. Phys. B **188**, 513 (1981); M. Dine, W. Fischler and M. Srednicki, Nucl. Phys. B **189**, 575 (1981); S. Dimopoulos and H. Georgi, Nucl. Phys. B **193**, 150 (1981); N. Sakai, Z. Phys. C **11**, 153 (1981); R. K. Kaul and P. Majumdar, Nucl. Phys. B **199**, 36 (1982).
- [2] S. Weinberg, Phys. Rev. D **13**, 974 (1976); L. Susskind, Phys. Rev. D **20**, 2619 (1979);
- [3] N. Arkani-Hamed, S. Dimopoulos and G. R. Dvali, Phys. Lett. B **429**, 263 (1998); I. Antoniadis, N. Arkani-Hamed, S. Dimopoulos and G. R. Dvali, Phys. Lett. B **436**, 257 (1998);
- [4] L. Randall and R. Sundrum, Phys. Rev. Lett. **83**, 3370 (1999); Phys. Rev. Lett. **83**, 4690 (1999).
- [5] J. C. Pati and A. Salam, Phys. Rev. D **10**, 275 (1974) [Erratum-ibid. D **11**, 703 (1975)]; H. Georgi and S. L. Glashow, Phys. Rev. Lett. **32**, 438 (1974).
- [6] M. B. Green, J. H. Schwarz and E. Witten, “Superstring Theory”, Vols. 1 and 2 (Cambridge University Press, Cambridge, 1987), and references therein.
- [7] J. Polchinski, “String Theory”, Vols. 1 and 2 (Cambridge University Press, Cambridge, 1998), and references therein.
- [8] T. Lin, PoS **333**, 009 (2019) [[arXiv:1904.07915 \[hep-ph\]](#)].
- [9] **PandaX-II** Collaboration, X. Cui et al., *Dark Matter Results From 54-Ton-Day Exposure of PandaX-II Experiment*, Phys. Rev. Lett. **119** (2017), no. 18 181302, [[arXiv:1708.06917](#)].
- [10] **LUX** Collaboration, D. S. Akerib et al., *Results from a search for dark matter in the complete LUX exposure*, Phys. Rev. Lett. **118** (2017), no. 2 021303, [[arXiv:1608.07648](#)].
- [11] **XENON** Collaboration, E. Aprile et al., *Dark Matter Search Results from a One Ton-Year Exposure of XENON1T*, Phys. Rev. Lett. **121** (2018), no. 11 111302, [[arXiv:1805.12562](#)].
- [12] A. Kurylov and M. Kamionkowski, Phys. Rev. D **69**, 063503 (2004) doi:10.1103/PhysRevD.69.063503 [[arXiv:hep-ph/0307185 \[hep-ph\]](#)].
- [13] F. Giuliani, Phys. Rev. Lett. **95**, 101301 (2005) doi:10.1103/PhysRevLett.95.101301 [[arXiv:hep-ph/0504157 \[hep-ph\]](#)].
- [14] S. Chang, J. Liu, A. Pierce, N. Weiner and I. Yavin, JCAP **08**, 018 (2010) doi:10.1088/1475-7516/2010/08/018 [[arXiv:1004.0697 \[hep-ph\]](#)].
- [15] Z. Kang, T. Li, T. Liu, C. Tong and J. M. Yang, JCAP **01**, 028 (2011) doi:10.1088/1475-7516/2011/01/028 [[arXiv:1008.5243 \[hep-ph\]](#)].
- [16] J. L. Feng, J. Kumar, D. Marfatia and D. Sanford, Phys. Lett. B **703**, 124-127 (2011) doi:10.1016/j.physletb.2011.07.083 [[arXiv:1102.4331 \[hep-ph\]](#)].

- [17] K. Hamaguchi, S. P. Liew, T. Moroi, and Y. Yamamoto, *Isospin-Violating Dark Matter with Colored Mediators*, JHEP **05** (2014) 086, [[arXiv:1403.0324](#)].
- [18] A. Drozd, B. Grzadkowski, J. F. Gunion, and Y. Jiang, *Isospin-violating dark-matter-nucleon scattering via two-Higgs-doublet-model portals*, JCAP **1610** (2016), no. 10 040, [[arXiv:1510.07053](#)].
- [19] M. T. Frandsen, F. Kahlhoefer, S. Sarkar, and K. Schmidt-Hoberg, *Direct detection of dark matter in models with a light Z'* , JHEP **09** (2011) 128, [[arXiv:1107.2118](#)].
- [20] G. Bélanger, A. Goudelis, J.-C. Park, and A. Pukhov, *Isospin-violating dark matter from a double portal*, JCAP **1402** (2014) 020, [[arXiv:1311.0022](#)].
- [21] V. M. Lozano, M. Peiró, and P. Soler, *Isospin violating dark matter in Stückelberg portal scenarios*, JHEP **04** (2015) 175, [[arXiv:1503.01780](#)].
- [22] X. Gao, Z. Kang, and T. Li, *Origins of the Isospin Violation of Dark Matter Interactions*, JCAP **1301** (2013) 021, [[arXiv:1107.3529](#)].
- [23] A. Crivellin, M. Hoferichter, M. Procura, and L. C. Tunstall, *Light stops, blind spots, and isospin violation in the MSSM*, JHEP **07** (2015) 129, [[arXiv:1503.03478](#)].
- [24] T. Li, Q. F. Xiang, Q. S. Yan, X. Zhang and H. Zhou, *Phys. Rev. D* **101**, no.3, 035016 (2020) [[arXiv:1908.00423](#) [hep-ph]].
- [25] H. Davoudiasl, R. Kitano, T. Li and H. Murayama, *Phys. Lett. B* **609**, 117-123 (2005) [[arXiv:hep-ph/0405097](#) [hep-ph]].
- [26] C. W. Chiang, J. Jiang, T. Li and Y. R. Wang, *JHEP* **12**, 001 (2007) [[arXiv:0710.1268](#) [hep-ph]].
- [27] B. C. Allanach and J. Davighi, *JHEP* **12**, 075 (2018) [[arXiv:1809.01158](#) [hep-ph]].
- [28] P. Minkowski, *Phys. Lett. B* **67**, 421-428 (1977)
- [29] T. Yanagida, in *Unified Theories*, eds. O. Sawada, et al., Feb., 1979; M. Gell-Mann, P. Ramond, R. Slansky, in Sanibel Symposium, CALT-68-709, Feb., 1979, and in *Supergravity*, eds. D. Freedman, et al. (Amsterdam, 1979); S. L. Glashow, in *Quarks and Leptons*, Cargese, eds. M. Levy, et al., pp.707, (Plenum, NY, 1980); R. N. Mohapatra and G. Senjanovic, *Phys. Rev. Lett.* **44**, 912 (1980).
- [30] T. Appelquist, B. A. Dobrescu and A. R. Hopper, *Phys. Rev. D* **68** (2003), 035012 doi:10.1103/PhysRevD.68.035012 [[arXiv:hep-ph/0212073](#) [hep-ph]].
- [31] F. Gursey, P. Ramond P. Sikivie, *Phys. Lett.* 60B(1976)177; Y. Achiman and B. Stech, *Phys. Lett. B*(1978)389; Q. Shafi, *Phys. Lett.* 79B (1978)301; P. Ramond, Caltech Preprint CALT-68-709(1979).
- [32] For a review, see, P. Langacker, *Rev. Mod. Phys.* **81**, 1199 (2009) [[arXiv:0801.1345](#) [hep-ph]].

- [33] J. Erler, Nucl. Phys. B **586**, 73 (2000).
- [34] P. Langacker and J. Wang, Phys. Rev. D **58**, 115010 (1998).
- [35] J. Erler, P. Langacker and T. Li, Phys. Rev. D **66**, 015002 (2002)
- [36] J. h. Kang, P. Langacker and T. Li, Phys. Rev. D **71**, 015012 (2005)
- [37] J. Kang, P. Langacker, T. j. Li and T. Liu, Phys. Rev. Lett. **94**, 061801 (2005) [hep-ph/0402086].
- [38] J. Kang, P. Langacker, T. Li and T. Liu, JHEP **1104**, 097 (2011)
- [39] E. Alvarez, M. Estévez and R. M. Sandá Seoane, [arXiv:2005.05194 [hep-ph]].
- [40] G. Aad *et al.* [ATLAS], Phys. Lett. B **796**, 68-87 (2019) doi:10.1016/j.physletb.2019.07.016 [arXiv:1903.06248 [hep-ex]].
- [41] R. Ajaj *et al.* [DEAP], Phys. Rev. D **100**, no.2, 022004 (2019) doi:10.1103/PhysRevD.100.022004 [arXiv:1902.04048 [astro-ph.CO]].
- [42] C. E. Yaguna, Phys. Rev. D **95**, no.5, 055015 (2017) doi:10.1103/PhysRevD.95.055015 [arXiv:1610.08683 [hep-ph]].
- [43] **Fermi-LAT** Collaboration, M. Ackermann *et al.*, *The Fermi Galactic Center GeV Excess and Implications for Dark Matter*, Astrophys. J. **840** (2017), no. 1 43, [arXiv:1704.03910].
- [44] **H.E.S.S.** Collaboration, H. Abdallah *et al.*, *Search for dark matter annihilations towards the inner Galactic halo from 10 years of observations with H.E.S.S.*, Phys. Rev. Lett. **117** (2016), no. 11 111301, [arXiv:1607.08142].
- [45] G. Belanger, F. Boudjema, A. Pukhov and A. Semenov, Comput. Phys. Commun. **176**, 367-382 (2007) [arXiv:hep-ph/0607059 [hep-ph]].
- [46] G. Belanger, F. Boudjema, A. Pukhov and A. Semenov, Comput. Phys. Commun. **185**, 960-985 (2014) [arXiv:1305.0237 [hep-ph]].